PHILIPPINE ENGINEERING JOURNAL
PEJ 2017; Vol. 38, No. 2: 43-62

Comparative Assessment of Water Column Correction Techniques for Seagrass Mapping Using Worldview-2 Image

Ayin M. Tamondong and Ariel C. Blanco
Department of Geodetic Engineering, College of Engineering, University of the Philippines- Diliman

Miguel D. Fortes
Marine Science Insititute, College of Science, University of the Philippines – Diliman

***Abstract*— Benthic cover mapping has always been challenging, primarily due to the compounding effects of the overlying water column. While a number of algorithms have been developed to address these, research on the application and performance assessment of such methods to seagrass mapping using high-resolution satellite images is limited. This research dealt with seagrass mapping using WorldView-2 images with an emphasis on the evaluation of the relative performance of different water column correction methods and on the band combinations. A geometric correction was conducted using DGPS survey coordinates. Atmospheric correction was performed using the Fast Line-of-Sight Atmospheric Analysis (FLAASH) model as this produced image-derived spectra similar to field spectra. Three water column correction models were applied and compared, namely, Lyzenga's Optical Model (LOM), Stumpf's Ratio Model (SRM), and Simple Radiative Transfer Model (SRTM). Maximum Likelihood Classification (MLC) was used to classify the image corrected for glint and water column effects. Using LOM and SRTM, overall classification accuracies obtained were 75.50% and 87.84%, respectively. STRM yielded the highest overall accuracy at 88.30% with ML applied on Worldview-2's coastal, green, yellow and red bands. However, the use of the coastal blue band, instead of the blue band, marginally increased the accuracy of the classification using SRTM.**

Keywords— seagrass, benthic habitats, mapping, WorldView-2

1. INTRODUCTION

The Philippines is composed of approximately 7,100 islands. It has one of the longest coastlines and most diverse coastal ecosystems in the world. Most of its people depend on marine and coastal biodiversity for their livelihood. Protection and proper management of coastal resources are important for a country like the Philippines. Currently, there is a lack of complete baseline data and inventory of coastal resources, particularly seagrasses, in the country.

Seagrasses are unique flowering plants [1], being the only angiosperms able to live completely submerged in water [2]. They produce flowers, fruits and seeds and they have an extensive rhizome system to anchor them firmly to the sea bottom [3]. Seagrass beds play an important role in marine environments. They are part of a complex ecosystem that supports different forms of life. They are food to several marine species [4]. Seagrasses also serve as breeding and nursery grounds, as well as habitat for fish and crustaceans [5]. Seagrasses also contribute to the physical structure of the environment. Sediments settle, as they pass through seagrass beds, settle stabilizing the seabed and reducing erosion. Seagrasses maintain coastal water quality and clarity. They help reduce greenhouse gases by absorbing carbon dioxide and they produce oxygen by photosynthesis [5]. Unfortunately, they are the most neglected coastal habitat. There are fewer research papers on seagrass than on corals. Priorities for studies or research are on other resources with immediate economic impacts, i.e., corals, seaweeds, animals, or fishes that either live in coastal habitats or are associated with them.

Assessment and monitoring our marine environment are essential for coastal resource management. Being able to map seagrasses augments our knowledge of seagrass ecology, emphasizes threats to seagrasses, and helps in finding ways to prevent possible losses and degradation [2]. Accurate, precise, and up to date information about the location and distribution of seagrasses is important for the sustainable preservation of the coastal ecosystem. Remote sensing techniques offer this capability in a cost-effective way, but it has its own set of limitations.

Airborne sensors were used for a long period to map seagrass ecosystems. With the availability of satellite-borne multispectral scanners in the 1970's, an alternative way of mapping emerged [6, 7]. Researches using moderate (Landsat TM, etc.) to high (Quickbird, IKONOS, etc.) resolution satellite images of mapping seagrasses materialized [8]. In 2003, an environmental remote sensing group in New South Wales used Landsat 5 TM and Landsat 7 ETM+ images to assess seagrass change from 1988 to 2002 in Wallis Lake. In this research, seagrass was distinguished from macroalgae and bare substrate. Mapping was carried out at spatial density that traditional in situ methodologies are unlikely to achieve. However, the authors suggested the use of Quickbird multispectral images for higher accuracy. [6]

The use of higher spatial resolution satellite imagery, including SPOT 5, IKONOS, Quickbird, and WorldView-2, would enable an increase in accuracy in mapping seagrasses. Pasqualini, et al. (2005) [9] used SPOT 5 to map a specific species of seagrass, *Posidonia oceanica* in the Mediterranean. Principal Components Analysis (PCA) was applied on the green (0.50 – 0.59 μm) and red (0.61 – 0.68 μm) bands of two SPOT 5 images and supervised classification by general hypercube was used to produce the cover map. They concluded that SPOT 5 has the potential for fine-level habitat discrimination, with an accuracy range of 73 – 96% comparable to that of IKONOS imagery. Arce (2005) [10] compared IKONOS and Hyperion for mapping benthic habitats, including seagrass. IKONOS is a high-resolution multispectral imagery with a 1m spatial resolution and 4 bands while Hyperion is a hyperspectral imagery with a 30m spatial resolution and 220 bands. Arce's results showed the benefits of using higher spatial resolution imagery when mapping benthic features [10]. Lyons, et al. (2011) [11] used Quickbird 4-band multispectral satellite imagery (spatial resolution of 2.44 m) to detect seagrass change cover in Moreton Bay, Australia. They were able to map and differentiate seagrasses using Maximum Likelihood supervised classification. However, with an overall accuracy of 63% only, it was concluded that the Quickbird sensor was not particularly suited for mapping discrete seagrass cover classes due to its wide spectral band range [11].

As noted, there have been many researches regarding the use of high-resolution multispectral satellite imagery to map seagrasses. However, further advancement is needed to obtain more accurate results. The WorldView-2 satellite imagery, having a 2.0 m spatial resolution for the multispectral bands and the inclusion of bands specific to coastal mapping, may enable more accurate seagrass mapping. Curran (2011) used PCA and ISODATA unsupervised classificationto detect seagrasses from three WorldView-2 images covering three study sites: Jarrett Bay, Blounts Bay, and Sandy Point. The satellite image of Sandy Point was found to be unusable for mapping seagrasses because of sun glint. The first 5 bands were subjected to PCA and components 1 and 2 of the PCA results were used for classification. Results showed that the water depth limit for accurately mapping seagrasses using remote sensing was less than 0.8 m. The accuracy results of the seagrass classification for Jarrett Bay were 40.9% for depths greater than 0.8 m, 86.4% for depths less than 0.8 m while for Blounts Bay, 50% for all depths. The low accuracies obtained are attributable to the lack of water column correction prior to image classification. Ludin and Ruslik (2011) [12] utilized two classification techniques: Maximum Likelihood per-pixel supervised classification and unsupervised classification after PCA on one satellite image. Spectral data of seagrass were used for accuracy assessment purposes. The combination of green, red-edge, and NIR2 bands produced significantly better seagrass detection compared with other band combinations. Ludin and Ruslik (2011) [12], unfortunately, was not able to map the extent of seagrass in the image due to the image being taken during high tide, but concluded that for depths less than 5 m, the accuracy of WorldView-2 to map seagrasses was more than 70%. Similar to Curran, no water column correction was applied. It is evident that without accounting for the effects of the water column, achievable seagrass mapping accuracy may be low.

The aim of this research is to develop a methodology to accurately map seagrasses and other benthic habitats of the coastal area around Santiago Island in Bolinao, Pangasinan using a WorldView-2 multispectral satellite image. In situ spectral data of seagrasses and other benthic covers, bathymetric data, field monitoring data on seagrasses, and actual knowledge of the study area were necessary. Recognizing the importance of water column correction, this research examines the performance of different water column correction techniques as applied to seagrass mapping.

2. MATERIALS AND METHODS

The study site is the coastal area surrounding Santiago Island, Bolinao, Pangasinan in the northwestern part of the Philippines (Figure 1). The coral reef system of Bolinao is typical of true fringing reefs in the Central Indo-Pacific [13] which experiences a maximum semi-diurnal tidal range of 1 m [14]. Similar to most of the reefs in the Philippines, the Bolinao reef system includes a significant area of seagrass beds. It has the most diverse seagrass beds in the Northern Philippines [15].

Figure 1. Seagrass meadows (dark green areas) surrounding Santiago Island, Bolinao, Pangasinan

Figure 2 shows the methodological framework of this research. The first step involves data gathering which includes acquiring the satellite image and conducting fieldwork, e.g., water quality surveys, bathymetric surveys, spectral measurements and establishment of ground control points. The processing of the satellite image involves geometric and radiometric correction, land masking, sun glint removal, and water column correction. After all these corrections, the image is classified. Accuracy assessment is then carried out using the validation data gathered before producing the final benthic habitat map.

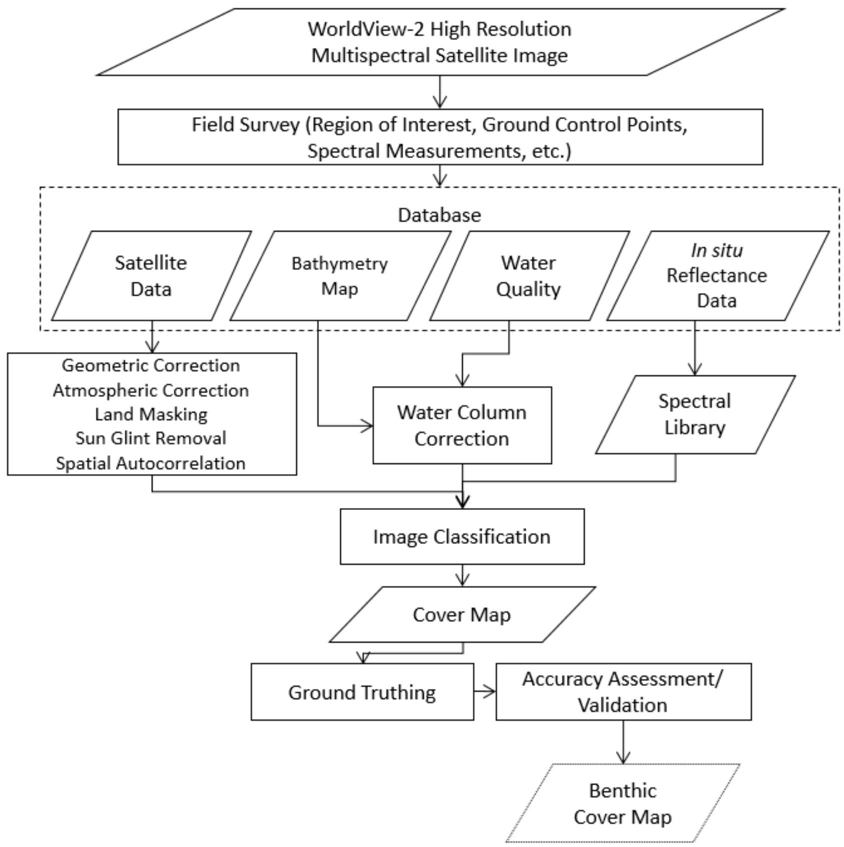

Figure 2. Benthic cover mapping methodology

Downwelling spectral irradiances, both in-air and underwater, were measured around Santiago Island on October 16, 2010, using a USB4000 Fiber Optic Spectrometer operating between 200 – 1100 nm with an optical resolution of ~0.3 (FWHM) and a 22-degree optical lens. To collect underwater irradiances, a 10-meter long fiber optic cable with a cosine diffuser was used at depths of less than a meter (except at the deep water station which is more than 10 m in depth). Irradiance is measured with the spectrometer pointing upwards with the cosine diffuser attached. A total of nine stations were established — six of them have seagrasses, one is a deep water location and the remaining two have other benthic covers such as corals, rubble, sand, seaweed (Figure 3). Water quality data were also measured at the different research stations using an AAQ Rinko to aid in the analysis of light attenuation. The AAQ measures depth, temperature, conductivity, salinity, turbidity, chlorophyll a, dissolved oxygen, pH and photo quantum. The positions of spectral measurement stations were determined using a Magellan handheld GPS receiver (nominal accuracy of 3 m).

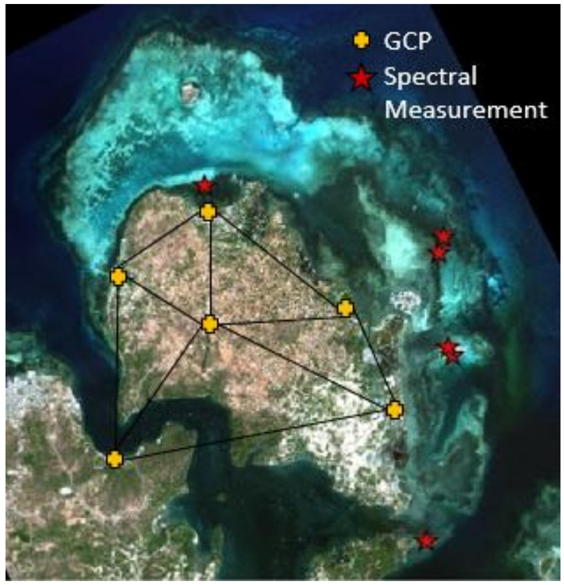

Figure 3. Ground control points (GCPs) indicated by yellow crosses and spectral data measurement sites indicated by red stars

Underwater irradiances were measured at different depths at one station to determine the attenuation coefficient of the water (Figure 4) to be used in the water column correction technique Simple Radiative Transfer Model. Irradiances above water were measured at every station to account for possible variations due to change in sun position, cloud cover, etc. The reflectance of seagrasses and other benthic covers was measured with the spectrometer with an approximate 45-degree angle from the zenith. Measurements of seagrasses were carried out above water, just below the water surface, mid-water, and at the bottom to obtain underwater spectral signatures of seagrasses and other benthic covers. To be able to calculate the optical leaf properties of seagrasses, samples were measured above water against an almost white and a black background. For each object, a total of 11 reflectances were measured and then averaged. All reflectance measurements were referenced to a calibrated white Labsphere Spectralon reference panel.

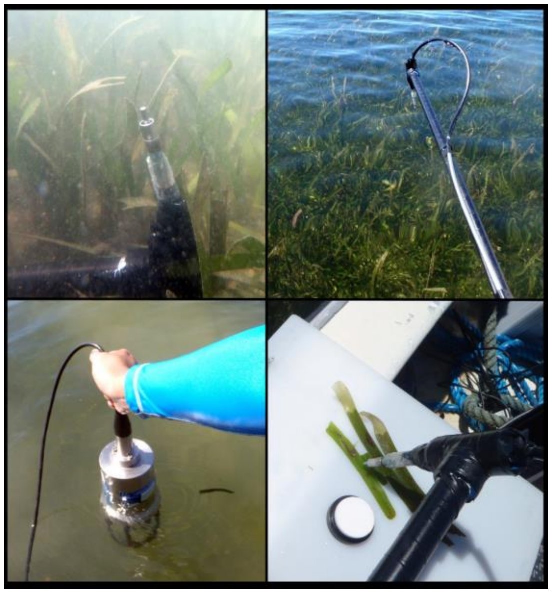

Figure 4. Fieldwork for spectral data measurement (Upper left: Measurement of underwater irradiance; *Upper right: Measurement of seagrass bed reflectance above water; Lower left: Water quality measurement using AAQ; Lower right: Reflectance measurement of seagrass samples.)*

Different benthic covers strategically located around Santiago Island were located in the field for use as training and validation data (Figure 5). Those areas with 70% to 100% seagrass cover are considered “dense seagrass areas”. Any area with less than 70% cover is considered “less dense seagrass” (Figure 6). These less dense seagrass areas are mostly seagrass mixed with sand and rubble. Corals and sargassum are located within the boundaries of the shallow area around the island.

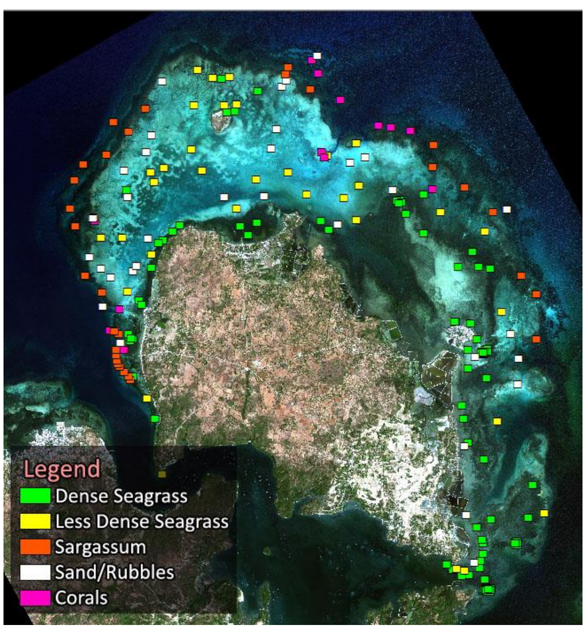

Figure 5. *In situ* benthic cover points of interest

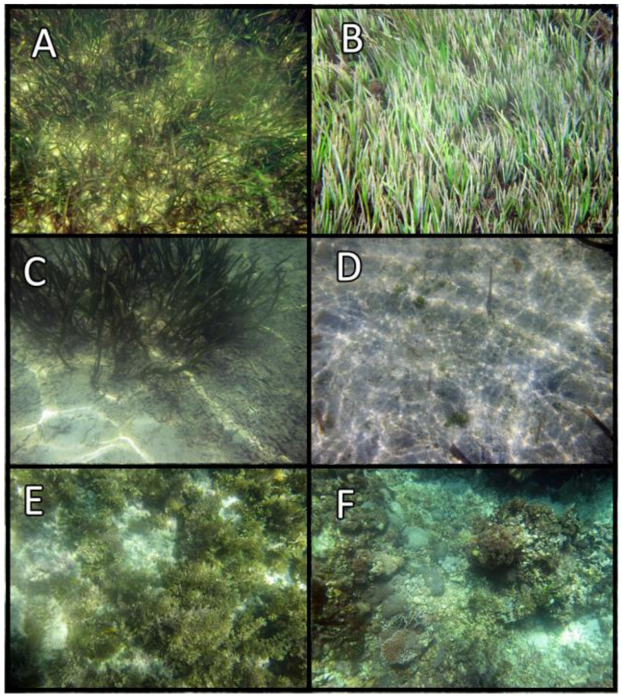

Figure 6. Photographs of different benthic covers: (A) and (B) Dense seagrass (C) Less dense seagrass (D) Sand (E) Sargassum (F) Corals.

Bathymetric data were obtained for use in the water column correction using the Stumpf's Ratio Model and Simple Radiative Transfer Model. ie. A Lowrance single-beam echosounder was used to acquire bathymetry data. The instrument was mounted on a boat which slowly cruised on a planned path around the study area. A HOBO water level logger was deployed to measure the change of tides during the survey. These data were then used to correct the bathymetry data. The HOBO water level data logger measures temperature and barometric pressure, from which water level at specified times can be computed. Point vector files were produced from the field survey data. An optical model implemented in ENVI 4.8 was then used to estimate the bathymetry from the image using the bathymetric data gathered from the field. The bathymetry and the water column optical properties are essential to the remote sensing of marine habitats, especially seagrass beds. Best results of the signal from the seagrass canopy are maximized by limiting the errors due to the attenuation of light in the water column [16].

Water quality data were also acquired in this research (Figure 4). The water column attenuates light that reaches the seagrass beds causing inaccurate spectral response from the benthos. Before reaching the substratum, light is attenuated by the depth of the water column itself and by five water column components. Light is either absorbed or scattered by pure water, colored dissolved organic matter (CDOM), phytoplankton, dead organic particulates, and mineral particulates [8]. To measure the water column components, AAQ, a cabled multi-parameter water quality meter, was used at several stations in the study area. It has sensors which measure conductivity, temperature, depth, chlorophyll fluorescence, turbidity, dissolved oxygen and pH [17].

The satellite image used in this research is a standard (LV2A) WorldView-2 multispectral image acquired on 7 March 2010. WorldView-2 high-resolution commercial imaging satellite captures images with eight multispectral bands: (1) coastal, (2) blue, (3) green, (4) yellow, (5) red, (6) red edge, (7) NIR1, and (8) NIR2. The coastal band (400 – 450 nm), said to be able to penetrate chlorophyll and water more than the blue band, was added to support vegetation analysis, bathymetric studies, and atmospheric correction techniques. The yellow band (585 – 625 nm), on the other hand, is significant for vegetation applications. The red edge band (705 – 745 nm) and near infrared 2 band (860 – 1040 nm) will aid in vegetation analysis. The spatial resolution is 1.84 m for the multispectral bands and is resampled to 2 m for commercially available images [17].

The satellite image was corrected for the following: radiometric, sensor, and geometric errors. The WorldView-2 Product Specifications states that WV2 geolocation accuracy is of 6.5 m CE90, with predicted performance in the range of 4.6 to 10.7 meters CE90, excluding terrain and off-nadir effects [19]. CE90 is defined as the horizontal accuracy. It is a measurement, expressed in meters, on the ground depicting the radius of a circle within which an object of known coordinates should be located on an image with an accuracy of 90% [19].

Ground control points (GCPs) were acquired to check the geometric correction of the image (Figure 3). In July 2010, six GCPs were measured using a Topcon HiPer Ga model receiver (DGPS) with a horizontal accuracy of 3 mm. Five of these GCPs were located on Santiago Island and one on the Bolinao mainland. Points on the island were positioned near the water boundaries to secure high accuracy for coastal areas. These GCPs were networked and adjusted accordingly. Using ENVI 4.8, image registration was applied on the image. A root mean square (RMS) error of 0.468 for an Image-to-Map registration was calculated. The image was resampled using the Nearest Neighbor 1st-degree Polynomial method. The Nearest Neighbor method was selected because it only moves original data values, meaning the digital number (DN) of the pixel nearest the resampled coordinates becomes the new DN of the output pixel [20]. It doesn't average pixel values making the image useable before atmospheric correction and classification. This is appropriate for mapping habitats because it preserves changes in data values across boundaries without smoothing them out. When extracting marine features, it is advantageous to remove all upland and terrestrial features, including clouds, [21, 22]; consequently, all upland features, were masked out of the image. The image explicit 0% cloud cover, eliminating the need for cloud masking.

Atmospheric correction removes the effects of the absorption and scattering of light in the atmosphere. This correction will result to the water-leaving radiance which is the measure of the total energy recorded from the top of the water column also known as at-surface-reflectance. In the case of marine remote sensing, only 8 to 10 percent of the signal corresponds to the marine reflectance. The total signal received at the satellite altitude is mostly by radiance contributed by atmospheric scattering processes [22, 23]. In this research, FLAASH (Fast Line-of-sight Atmospheric Analysis of Spectral Hypercubes) was used for atmospheric correction. FLAASH incorporates the MODTRAN4 radiation transfer code. This model begins with a standard equation for spectral radiance at a sensor pixel, L, involving the addition of the radiance that is reflected from the surface and goes straight into the sensor and the radiance from the surface that is scattered by the atmosphere and into the sensor.

Sun glint correction is vital to attain more accurate mapping of benthic features. Sunglint is the specular reflection of light from water surfaces [24] caused by ocean swell and chops, thereby limiting the quality and accuracy of benthic remote sensing [25, 26]. It is a function of sea surface state, sun position, and viewing angle. The deglinting method of Hocheberg, et al. (2003) refined by Hedley, et al. (2005) was applied in this research. Pixels that exhibit different ranges of sun glint, preferably over deep water areas, were selected. From the selected pixels, the minimum near infrared value (minNIR) was determined. This value represents the NIR brightness with no sun glint. A linear regression of NIR brightness (x-axis) against the band signal (y-axis) was then implemented. The slope of this regression line is the output of interest (bi). Subtracting the product of bi and the NIR brightness of the pixel resulted in the deglinted image band [26]. This was applied to all bands. Figure 7 shows the image before and after sun glint correction.

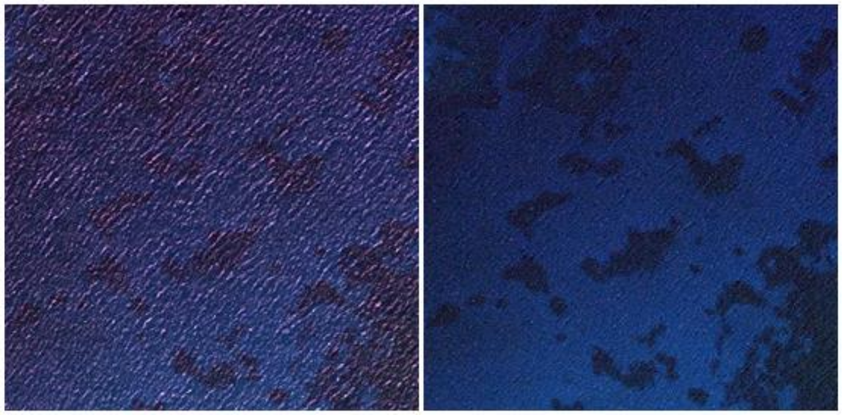

Figure 7. Before (left) and after (right) sun glint correction

Lastly, water column correction was also applied to the image. As noted earlier, previous researches on seagrass mapping have neglected the potential impact of the water column on classification accuracy. In this research, three water column correction methods, namely, Lyzenga's Optical Model (LOM), Stumpf's Ratio Model (SRM), and a simple radiative transfer model (SRTM), were examined.

The Lyzenga's Optical Model, also known as Linear Band Model, is an image-based water column correction technique. To remove the influence of depth on the bottom reflectance, a measurement of depth for every pixel in the image and information of the attenuation characteristics of the water column are required [27]. It is, however, difficult to provide depth measurements for each image pixel. LOM addresses this using a 'depth invariant bottom index' generated from each pair of spectral bands to remove the effects of the water column in the image without the need to measure water depth. LOM requires prior removal of scattering in the atmosphere and external reflection from the water surface (sun glint).

In clear waters, light decays exponentially with increasing depth. In this algorithm, to make the relationship of the radiance and depth linear, values of radiances are transformed using natural logarithms (ln).

$$X_i = \ln(L_i) \tag{1}$$

In Equation 1, X_i is the transformed radiance of a pixel in band i, and L_i is the pixel radiance in band i, which should already be corrected for atmospheric effects and sun glint. Groups of pixels of the same bottom types but of varying depths are then selected from the image bands which exhibit attenuation and have good water penetration.

The severity of light attenuation in the water is described by the attenuation coefficient, k. Solving for k requires calculation of too many unknown quantities, making this unfeasible. Lyzenga addressed this problem by using information from more than one band. Getting the ratio of attenuation coefficients cancels out unknown parameters. To calculate the ratio of attenuation coefficient, k_i/k_j, two bands are selected and a bi-plot of log transformed radiances for the same bottom types but varying depths is made. The slope of the bi-plot represents the ratio of attenuation coefficients between bands. This ratio k_i/k_j is dependent only on the wavelength of the band and clarity of the water and is independent of the bottom type. The slope represents an axis of radiance values for a specific substratum. Only depth changes as one moves along the line.

Adding a bi-plot of radiance values of a different bottom type would yield a similar line with only depth changing between data points. However, this line would not lie on the exact same position as the other bottom type. It will be displaced either above or below the bi-plot of the first bottom type because of the difference in radiance values between different bottom types but nevertheless, the gradient of each line should be identical. To obtain the index of each bottom type, the y-intercept must be calculated. From the equation of a line:

$$Y = p + q * x, \tag{2}$$

Where p is the y-intercept and q is the gradient of the regression of y on x.
Solving for the y-intercept, p:

$$P = Y - q * x, \tag{3}$$

Consequently, the depth invariant index can be obtained as follows:

$$\text{depth invariant index}_{ij} = \ln(L_i) - \left[\left(\frac{k_i}{k_j}\right)\ln(L_i)\right], \tag{4}$$

This algorithm, however, cannot account for varying bottom types without extensive calibration. It must be used on a uniform substrate, hence, the need to identify in the image different substrate types and apply the algorithm separately on each type. Furthermore, it should be noted that LOM's major weakness is that it is dependent on the clarity of the water.

In 2003, Stumpf and Holderied [28] presented an alternative bathymetry algorithm which better accounts for water turbidity. The SRM provided a solution for water column correction with fewer parameters, thus, making it easier to apply on large areas of interest. Atmospheric correction is required prior to the application of the ratio model. Similar to LOM, transformed natural logarithms of radiance values were used to linearize the relationship between band spectral values and depth. A simple linear relationship between the ratio of reflectance in two bands and depth were used instead of a multiple linear regression.

Different bands have different water absorption characteristics. This means one band will have less reflectance values than the other. Bands with higher absorption will have reflectance values that will decrease proportionally faster than bands with lower absorption. Accordingly, the ratio between the low and high absorption bands will increase when both are log-transformed. Change in ratio because of change in albedo is much less than that caused by change in depth signifying that dissimilar bottom albedos will still have the same ratio at constant depth. This being said, the ratio may be used to approximate depth independently of substrate and needs only to be scaled to the actual depth using the equation:

$$Z = m_1 \frac{\ln(n\,L_i)}{\ln(n\,L_j)} - m_0, \tag{5}$$

where m_1 is a tunable constant representing the slope of the relationship between the ratio and depth, n is a fixed constant for all areas to guarantee positive logarithm values and a linear response with depth, and m_0 is an offset for depth (Z=0). Unfortunately, this algorithm could not take into account the varying albedo over seagrass substrate, similar to the limitation of the LOM.

Another method to determine the bottom reflectance is the use of a simplified radiative transfer model (SRTM) of light to correct for the effects of the water column. Reflectance at the water surface is equal to the sum of the contribution of the bottom and the water column. The deeper the water, the lesser is the contribution of the bottom to the water surface reflectance. Consequently, the shallower the depth, the more negligible is the contribution of the water column and the greater is the contribution of the bottom [29]. The reflectance at the water surface was modelled using *in situ* spectral measurements as follows [29]:

$$R_{o-}(\lambda_i) = R_\infty(\lambda_i) * \left(1 - e^{(-2K_d z)}\right) + R_b(\lambda_i) * \left(e^{(-2K_d z)}\right) \tag{6}$$

Where:

$R_{o-}(\lambda_i)$ = 0.545 * $R_{o+}(\lambda_i)$ is the spectral reflectance just below the water surface;

$R_{o+}(\lambda_i)$ is the spectral reflectance just above the water surface;

$R_\infty(\lambda_i)$ is the spectral reflectance of an infinitely deep homogeneous water column;

$R_b(\lambda_i)$ is the bottom spectral reflectance;

$K_d(\lambda_i)$ is the diffuse attenuation coefficient, and;
z is the water depth

A spectral parameter, K_d, which is the diffuse attenuation coefficient is used to determine the depth at which a water column can be considered optically infinite. It was computed directly from in situ underwater measurements of downwelling spectral irradiance using the equation:

$$K_d(\lambda, z) = \frac{ln\frac{E_d(\lambda z_1)}{E_d(\lambda z_2)}}{z_2 - z_1}, \tag{7}$$

where c $(\lambda, z_1)$and v (λ, z_2) are the in situ downwelling spectral irradiance at depths z1 and z2 below the water surface, respectively.

After all the corrections have been applied, Maximum Likelihood Classification (MLC), which uses the variance and covariance in class spectra to determine the classification scheme, was used to classify the image corrected using the three water column correction techniques, namely: Lyzenga's Model, Stumpf's Ratio Model and the Simplified Radiative Transfer Model. Classified images from different band combinations, 1 (coastal) 3 (green) 4 (yellow) 5 (red), 2 (blue) 345, 13456 (red edge) and 23456, were also produced. Field data were used to create the regions of interest of different benthic covers such as dense seagrass, less dense seagrass, corals, sargassum, and sand. Accuracy assessment of the classified images was carried out using the field validation data.

3. RESULTS

3.1 Irradiance and Spectral Reflectance

The irradiance across the spectral range decreases as the depth or the overlying water column height increases (Figure 8). Attenuation is relatively low in the 400 – 500 nm range and beyond 900 nm. The decrease is greatest in the 500-700 nm range. Water absorbs more in the 600 – 700 nm range, where WorldView-2's red band (630 – 690 nm) lies. Yang [30] also observed the absorption of an optically shallow water in the 600 – 800 nm range. On the other hand, water absorbs minimally in the shorter wavelengths, including WorldView-2's coastal band (400 – 450 nm) and blue band (450 – 510 nm). Consequently, the reflectance of different benthic covers would decrease as measurements are taken deeper into the water column.

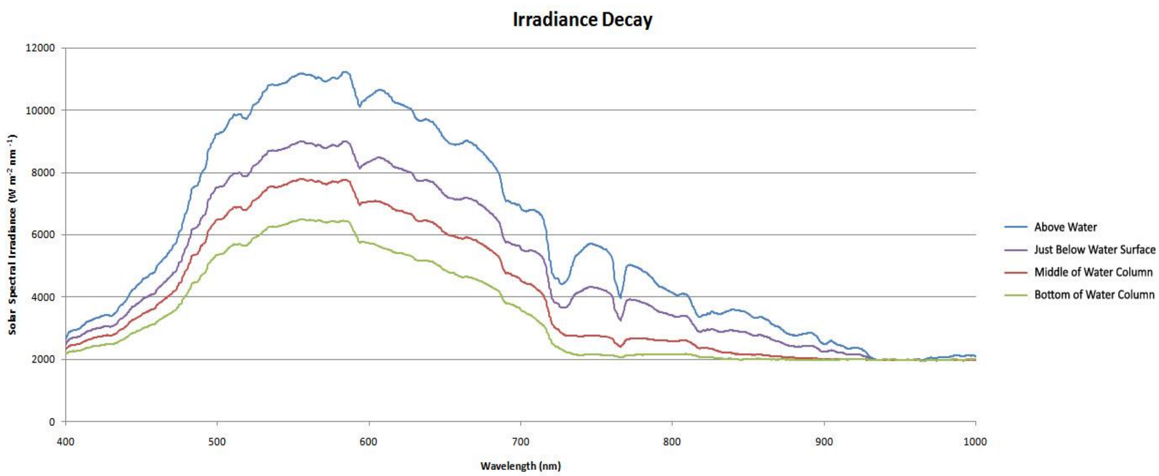

Figure 8. Irradiance decay as it goes deeper into the water column measured using a spectroradiometer

Seagrass, sand, coral, and rock are most separable in the 500 – 650 nm range, which covers the green, yellow, and red bands (Figure 9). In contrast, these cover types are least discernible in regions beyond 700 nm. Rocks and corals are inseparable in the 400-450nm range. Sand has the most distinctly separate spectral signature, having the highest reflectance in the visible range. Seagrass has the lowest reflectance. In view of these observations, the coastal, blue, green, yellow and red bands (Bands 1, 2, 3, 4, 5, respectively) are considered the most suitable bands for mapping benthic habitats. This is consistent with Yang [30], who observed that 555, 650, 675 and 700 nm are good bands for estimating the leaf area index (LAI) of seagrasses and concluded that 500 – 630 nm and 680 – 710 nm are the most effective ranges for classifying seagrass. Zaffoli et al. [31] also observed that the bands between 400 – 600 nm are best to use for bottom classification while Misbari et al. [32] found that the blue and red bands of Landsat TM and OLI have the highest agreement between field data and seagrass delineation.

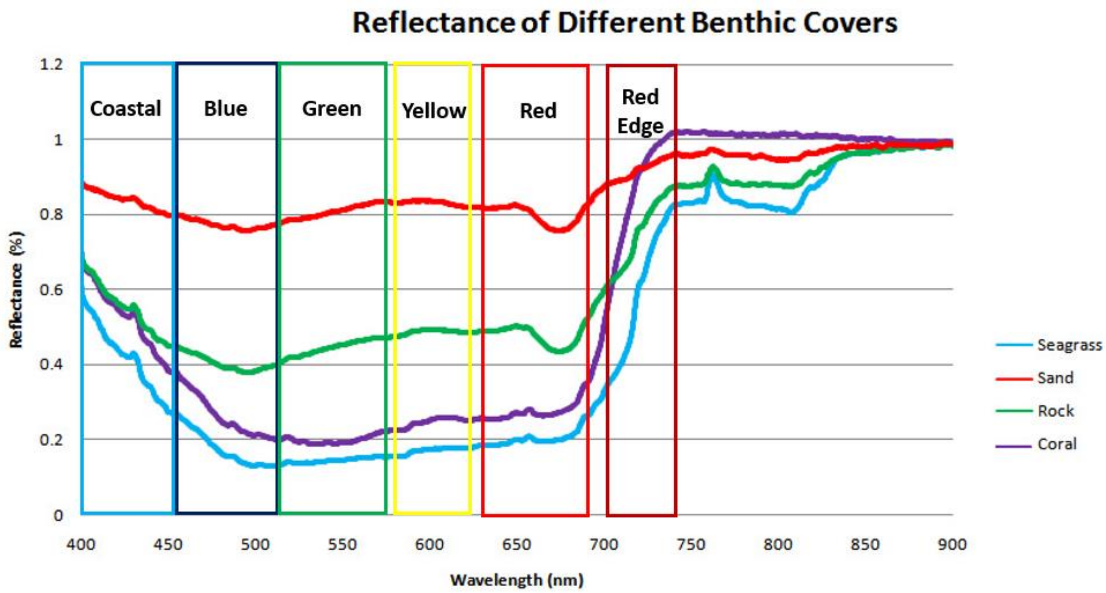

Figure 9. Comparison of underwater reflectance values of different benthic covers with the corresponding band ranges of WorldView-2

3.2 Comparative Performance of Water Column Correction Techniques

Comparing overall accuracies of different classification images (Table 1) from different water column correction techniques with varying band combinations showed that the Simplified Radiative Transfer Model (SRTM) and Stumpf's Ratio Model (SRM) have almost equal accuracies. The SRTM produced the highest overall accuracy with 88.30% using the coastal, green, yellow and red bands while SRM's overall accuracy was 87.84%. The lowest overall accuracies were obtained using Lyzenga's Optical Model (LOM) across different band combinations. The use of the coastal band instead of the blue band resulted in a minimal increase in overall accuracy when SRTM and SRM are applied. This is not the case for LOM, which even resulted in significantly lower overall accuracy. LOM does not require field data, making it the easiest water column correction to apply. However, it is effective only in clear waters [31]. This is not the case in many parts of the study area, hence, the relatively poor performance of the LOM.

Table 1. Overall Classification Accuracy Obtained with Different Water Column Correction Techniques

Water Column Correction Model	***Band Combinations***			
	1345	**2345**	**13456**	**23456**
Lyzenga's Optical Model (LOM)	75.54%	82.04%	69.39%	74.11%
Stumpf's Ratio Model (SRM)	87.84%	86.70%	86.73%	86.05%
Simple Radiative Transfer Model (SRTM)	88.30%	87.29%	86.98%	85.96%

The spatial distributions of benthic cover as mapped using SRM and SRTM are highly similar while that of LOM is noticeably different (Figure 10). There were more "sargassums" mapped using LOM. These included actual dense seagrass areas in the north of Santiago Island and north of the mainland

Bolinao. LOM yielded low user’s accuracy (23.54%) for sargassum (Table 2). Dense and less dense seagrass have relatively high producer’s and user’s accuracy (61.83% – 98.25%) across the three water column correction techniques with the lowest being the producer’s accuracy using LOM. Corals have relatively low producer’s and user’s accuracy (42.38% – 56.68%). Corals are typically located in optically deeper waters than seagrasses. As such, classification resulted in a lower accuracy because the contribution of the bottom diminishes as the depth increases [31]. It becomes difficult to differentiate bottom reflectance in deeper waters causing confusion between corals and other covers. SRTM produced the highest overall accuracy but it wasn’t the highest producer’s or user’s accuracy of some benthic covers. For corals, SRM had the highest producer’s (56.68%) and user’s (52.76%) accuracy because the efficiency of SRTM is reduced in deeper waters. For other classes, the producer’s or user’s accuracy of LOM and SRM are at times higher than SRTM. SRTM takes into account the quality of water in the area thus assuming an attenuation coefficient uniform in the study area, resulted to lower accuracies of SRTM.

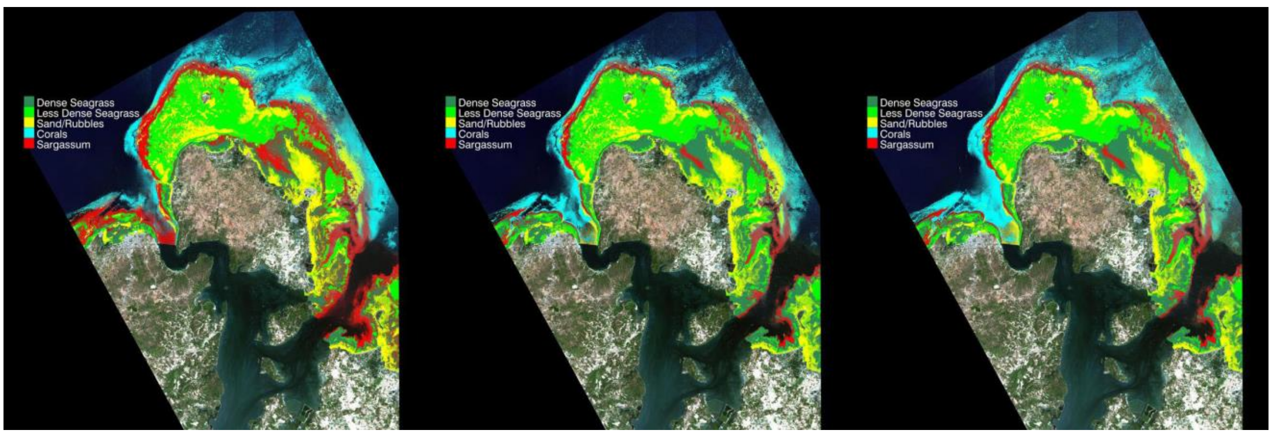

Figure 10. Maximum Likelihood Classified Images with Band Combination 1,3,4,5 (from left to right) using Lyzenga’s Optical Model, Simple Radiative Transfer Model (SRTM) and Stumpf’s Model

Table 2. Producer’s and User’s Accuracy of the Classified Images Corrected for Water Column Effects using Different Techniques for Bands 1, 3, 4, 5

Class	Lyzenga's Optical Model		Stumpf's Ratio Model		Simple Radiative Transfer Model	
	Producer's Accuracy (%)	User's Accuracy (%)	Producer's Accuracy (%)	User's Accuracy (%)	Producer's Accuracy (%)	User's Accuracy (%)
Corals	46.35	49.49	56.68	52.76	42.38	51.06
Dense Seagrass	61.83	98.25	87.90	96.52	88.07	96.38
Less Dense Seagrass	87.78	83.1	90.3	81.51	91.84	82.15
Sand	87.99	70.33	83.06	71.53	80.22	81.64
Sargassum	85.42	23.54	71.23	51.73	72.5	47.49

3.3 Coastal Blue (Band 1) vs. Blue (Band 2)

Comparing SRM classification images based on separate use of coastal band and blue band shows minimal visible differences (Figure 11). This corresponds to the comparable overall accuracies noted earlier. Based on spectral signatures (Figure 9), seagrass, corals, and sand have good separability in both coastal and blue band ranges. The producer's and user's accuracy (Table 3) of the coral, dense seagrass and less dense seagrass indicate minimal increase with the use of the coastal blue band. Significant increases in user's and producer's accuracy were noted for sargassum. Though the accuracies for sand slightly decreased, the use of the coastal band produced the highest overall accuracy at 87.84%.

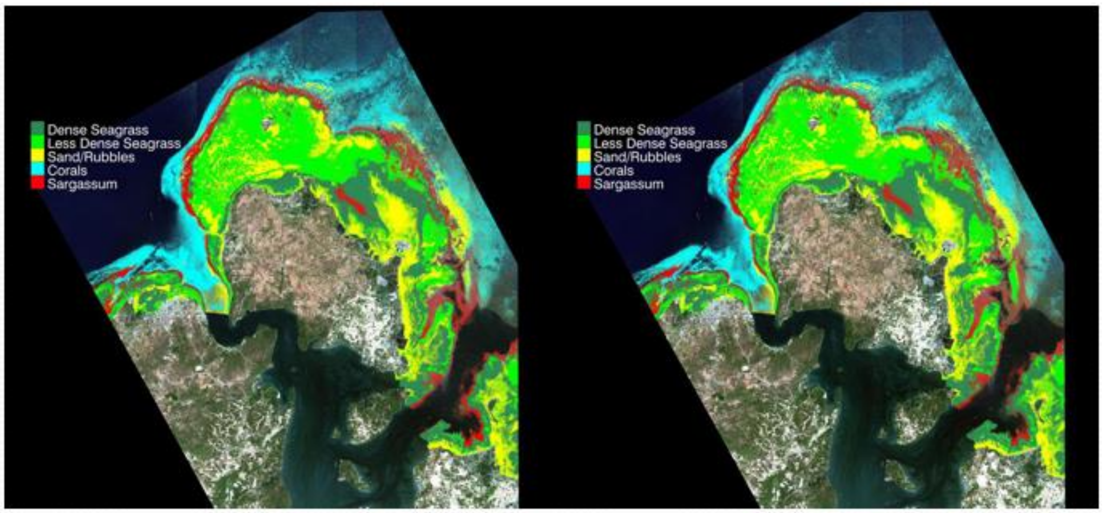

Figure 11. Classified Images of Stumpf's Ratio Model using *Band Combination 1, 3, 4, 5 (left) and 2, 3, 4, 5 (right)*

Table 3. Producer's and User's Accuracy of Stumpf's Ratio Model with *Band Combination 1, 3, 4, 5 and 2, 3, 4, 5*

Class	Band Combination 1, 3, 4, 5		Band Combination 2, 3, 4, 5	
	Producer's Accuracy (%)	User's Accuracy (%)	Producer's Accuracy (%)	User's Accuracy (%)
Corals	56.68	52.76	56.68	49.65
Dense Seagrass	87.90	96.52	85.86	95.79
Less Dense Seagrass	90.30	81.51	90.11	82.37
Sand	83.06	71.53	84.52	74.5
Sargassum	71.23	51.73	66.08	45

3.4 Use of Red Edge

Adding the red edge (band 6) decreased the overall accuracy of all classified images (Table 1). However, the decrease is only pronounced for the LOM-based classification images. The reflectance curves of the different benthic cover classes, except seagrass, are overlapping with each other in the wavelength range of the red edge band (705 – 745 nm). This has produced depth invariant index layers with reduced separability among classes, resulting to lower LOM accuracy. For the case of SRM and STRM, it is evident that the red edge did contribute additional significant information for the separation of the classes.

4. DISCUSSION

Remote sensing has been an effective tool in mapping seagrasses in recent years. However, to compensate for the effects of the water column, correction techniques are essential to increase the accuracy of classification from satellite images. The water column attenuates light especially in the longer wavelengths and increasing depths, making it difficult to retrieve bottom reflectance from satellite images. The use of water column correction techniques minimizes these effects. There are different water column correction techniques; three were implemented in this research.

The advantage of Lyzenga's Optical Model (LOM) is that it uses the ratio of bands with good water penetration to lessen the effects of the water column. Field data are not required to use the model, making it the easiest method among the three. However, based on the results presented herein, it gave the lowest overall accuracy (see Table 1). The assumption of LOM is that the water is clear and uniform in the study area which is not the case in most areas with seagrasses. This limits the application of LOM in seagrass mapping. In addition, LOM requires sample areas with homogeneous cover type. This may not be a problem with high resolution images but may be an issue when using LOM on lower resolution images (e.g., Landsat).

Stumpf's Ratio Model (SRM) is an improvement of LOM. It makes use of actual depth data or estimates to improve the approximation of the water column's influence on light penetration. This added feature improved the accuracy of the classification of seagrass and other benthic habitats compared to that of LOM (Table 3) while maintaining relative ease of application. However, as pointed out earlier, both LOM and SRM are unable to account for varying albedos. Hence, sample areas must be carefully selected. Furthermore, the performance of SRM may vary depending on the number and location of depth measurements or estimates to fine-tune the approximation process. In this research, depths throughout the study were estimated using bio-optical modelling, thereby the approximation can be made with reasonable accuracy throughout the study area. It can be argued that the requirement for actual depth values may limit the application of SRM. However, tools for bathymetric estimation has become increasingly available, for example the BOMBER (Bio-Optical Model Based tool for Estimating water quality and bottom properties from Remote sensing images), an add-on tool for ENVI+IDL [33] which is based on the works of Albert and Mobley (2003) [34] and Lee et al. (1998) [35].

The highest overall accuracy was produced by the Simple Radiative Transfer Model. SRTM needs intensive field data. Information needed from the field is reflectance of an infinitely deep water, surface reflectance, bottom reflectance, depth and attenuation coefficient. With these, the SRTM can accurately account for the effects of the water column. However, these measurements are typically not available.

The unavailability of a spectrometer and the difficulty of spectral measurements may pose a challenge towards widespread use of SRTM. It was pointed out that this additional information only slightly increased the accuracy of classification compared to the results of SRM.

Table 4. Comparison of water column correction techniques

	Lyzenga's Optical Model	Stumpf's Ratio Model	Simple Radiative Transfer Model
Needs Depth Data	*No*	*Yes*	*Yes*
Needs Field Spectrometry Data	*No*	*No*	*Yes*
Attenuation Coefficient	*Image-based*	*Image-based*	*Field-based*

Table 4 summarizes the differences in the application of the water column correction techniques used in this research. LOM doesn't require field data while SRM requires depth data and SRTM requires depth and field spectrometry data. The attenuation coefficients of LOM and SRM are estimated from band ratios of the image while SRTM needs the actual attenuation coefficient from field data. Based on the results, SRM is a suitable alternative to SRTM, considering similar accuracy levels obtained. SRM may even be preferred over SRTM considering relative ease of application. However, SRM and SRTM will have to be applied and compared in other sites with different water quality conditions.

WorldView-2 satellite imagery boasts of its coastal band for mapping coastal features because of its ability to penetrate the water better than the other bands. The use of the coastal band instead of the blue band slightly increased the overall accuracy of benthic habitats. It produced the highest overall accuracy at 87.84%, with notable improvement in mapping sargassum. This is considered significant as sargassum and seagrass are typically difficult to accurately separate in satellite images. On the other hand, the use of red edge band, which is valuable in vegetation studies, was shown to decrease the overall accuracy of classification. This is consistent with the findings of Yang et al., [36] that although seagrasses have high reflectance in the red edge range, there is a poor correlation between the subsurface remote sensing reflectance at 715 nm and leaf area index (LAI) because of the absorption of water in this range.

5. CONCLUSIONS

The research has evaluated the performance of water column correction techniques through the assessment of the accuracy of the resulting benthic cover classification. The combination of coastal blue, green, yellow, and red is the best combination to use for mapping benthic cover based on WorldView-2 images. However, the use of coastal blue instead of the blue band offered marginal improvements in the classification accuracy. As shown in this research, the Simple Radiative Transfer Model and the Stumpf's Ratio Model produced comparably accurate results. In contrast, the Lyzenga Optical Model performed poorly as it cannot account for the spatial variability in water column characteristics. Adding the red band did not result in significant improvement in the classification. To the contrary, it worsened the classification accuracy when the Lyzenga Optical Model was used.

Among the water column correction techniques implemented in this research, the Simplified Radiative Transfer Model showed the best classification with an overall accuracy of 88.30%. The SRTM takes into account in situ light attenuation data of the study area. It uses a diffuse attenuation coefficient computed from actual underwater measurements of downwelling spectral irradiance. Due to comparable accuracy and practicality, the SRM can be considered as a good alternative model. Overall, Worldview-2 is suitable for mapping seagrasses provided the effects of the atmosphere, sun glint, and water column are properly accounted for.

6. REFERENCES

[1] Kuo, J.; McComb, A. J. Seagrass taxonomy, structure and development. In *Biology of seagrasses : a treatise on the biology of seagrasses with special reference to the Australian region;* Larkum, A.W.D., McComb, A.J. and Shephard, S.A., Eds.; Elsevier Science Pub.: Amsterdam, The Netherlands, 1989**,** pp. 6 – 73.

[2] Polina, L. *Seagrass mapping and monitoring along the coasts of Crete, Greece*, LAP Lambert Academic Publishing, 2011; 180pp., ISBN-13: 978-3846535165.

[3] McKenzie, L. J., *Seagrass-Watch. Proceedings of a Workshop for Mapping and Monitoring Seagrass Habitats in North East Arnhem Land, Northern Territory*, Seagrass-Watch HQ, Cairns, 2008; 49pp.

[4] PNSC, *Seagrasses of the Philippines: Country Report/ UNEP/GEF SCS Project: Reversing Environmental Degradation Trends in the South China Sea and Gulf of Thailand*, Philippine National Seagrass Committee (PNSC) Publ. Philippines, 2004.

[5] Seagrass Booklet. Available online: http://www.ioseaturtles.org/Education/seagrassbooklet.pdf. (accessed on 31 March 2012).

[6] Ferguson, R. L.; Korfmacher, K. Remote Sensing and GIS analysis of seagrass meadows in North Carolina, USA. *Aquatic Botany* **1997,** *Volume 58*, pp. 241 – 258, DOI: 10.1016/S0304-3770(97)00038-7

[7] Ferwerda, J. G.; Leeuw, J. D.; Atzberger, C.; Vekerdy, Z. Satellite-based monitoring of tropical seagrass vegetation: current techniques and future developments. *Hydrobiologia* **2007**, Volume 591, pp. 59 – 71, DOI: 10.1007/s10750-007-0784-5

[8] Dekker, A. G.; Brando, V. E.; Anstee, J. M.; Fyfe, S.; Malthus, T.; Karpouzli, E. Remote Sensing of Seagrass Ecosystems: Use of Spaceborne and Airborne Sensors. In *Seagrasses: Biology, Ecology and Conservation*, Springer, Dordrecht, 2007; pp. 347 – 359, ISBN: 978-1-4020-2983-7.

[9] Pasqualini, V.; Pergent-Martini, C.; Pergent, G.; Agreil, M.; Skoufas, G.; Sourbes, L.; Tsirika, A. Use of SPOT 5 for mapping seagrasses: An application to *Posidonia oceanica*. *Remote Sensing of Environment*, Elsevier **2004**, *Volume 94*, pp. 39 – 45, DOI: 10.1016/j.rse.2004.09.010

[10] Arce, J. Remote Sensing of Benthic Habitats in Southwestern Puerto Rico. Master of Science, University of Puerto Rico, Puerto Rico, 2005.

[11] Lyons, M.; Phinn, S.; Roelfsma, C. Integrating Quickbird Multi-Spectral Satellite and Field Data: Mapping Bathymetry, Seagrass Cover, Seagrass Species and Change in Moreton Bay, Australia in 2004 and 2007. *Remote Sensing* **2011,** *Volume 3*, pp. 42 – 64, DOI: 10.3390/rs3010042.

[12] Ludin, A. N. M.; Ruslik, N. R.; Mapping of Seagrass along Sunghai Pulai, Johor, Malaysia. Digital Globe WorldView-2 8 Band Research Challenge, 2011

[13] McManus, J.; Nanola, C.; Reyes, R.; Kesner, K.; *Resource Ecology of the Bolinao Coral Reef System*; International Center for Living Aquatic Resources Management: Manila, Philippines, 1992; ISBN 971-8709-28-2.

[14] Vermaat, J.; Agawin, N.; Duarte, C.; Fortes, M.; Marba, N.; Uri, J. Meadow maintenance, growth and productivity of a mixed Philippine seagrass bed. *Marine Ecology Progress Series* **1995,** *Volume 124*, pp. 215 – 225, DOI: 10.3354/meps124215.

[15] Fortes, M.; Go, A.; Bolisay, K.; Nakaoka, M.; Uy, W.; Lopez, M.; Leopardas, V.; Leriorato, J.; Pantallano, A.; Paciencia, F.; Watai, M.; Honda, K.; Edralin, M. Seagrass response to mariculture-induced physio-chemical gradients in Bolinao, northwestern Philippines. Proceedings of the 12th International Coral Reef Symposium, Cairns, 2012.

[16] Dekker, A. G.; Brando, V. E.; Anstee, J. M.; Pinnel, N.; Kutser, T.; Hoogenboom, E. J.; Peters, S.; Pasterkamp, R.; Vos, R.; Olbert, C.; Malthus, T. J. Imaging Spectrometry of Water, In *Imaging Sectrometry. Remote Sensing and Digital Image Processing*; Meer F. D., Jong S. M. D., Eds.; Springer, Dordrecht, 2002; pp. 307 – 359, ISBN 978-0-306-47578-8.

[17] Analytical Solutions. Available online: http://www.analyticalsolns.com.au/product/aqua_quality_meter.html (accessed on 24 August 2017).

[18] Updike, T.; Comp, C. Radiometric Use of WorldView-2 Imagery. DigitalGlobe, Colorado, USA, 2010.

[19] Costa, J. K. N. D.; Agnieszka, W. Geometric Quality Testing of the WorldView-2 Image Data Acquired over the JRC Maussane Test Site using ERDAS LPS, PCI Geomatics and Keystone digital photogrammetry software packages – Initial Findings. Publications Office of the European Union, 2010; DOI: 10.2788/83409

[20] Green, E. P.; Mumby, P. J.; Edwards, A. J.; Clark, C. D. *Remote Sensing Handbook for Tropical Coastal Management*. UNESCO Publishing: Paris, France, 2000; ISBN 92-3-103736-6.

[21] Jensen, J.; Narumalani, S.; Weatherbee, O.; Mackey, H. Remote Sensing offers an alternative for mapping wetlands. *GeoInformation Systems* **1991**; pp. 46 – 53.

[22] Mishra, D.; Narumalani, S.; Lawson, D.; Rundquist, M. Benthic Habitat Mapping in Tropical Marine Environments Using Quickbird Multispectral Data. *Photogrammetric Engineering & Remote Sensing* **2006,** *Volume 72*, p. 1037 – 1048.

[23] Kirk, J. T. O. *Light and Photosynthesis in Aquatic Ecosystems*, 3rd ed.; Cambridge University Press: Cambridge, UK, 2011; ISBN 978-0-521-15175-7.

[24] Kay, S.; Hedley, J. D. Lavender, S. Sun Glint Correction of High and Low Spatial Resolution Images of Aquatic Scenes: a Review of Methods for Visible and Near-Infrared Wavelengths. *Remote Sensing* **2009,** *Volume 1*, pp. 697 – 730, DOI: 10.3390/rs1040697.

[25] Hochberg, E.; Andrefouet, S.; Tyler, M. Sea surface correction of high spatial resolution Ikonos images to improve bottom mapping in near-shore environments. *IEEE Transactions on Geoscience and Remote Sensing* **2003**, *Volume 41***,** pp. 1724 – 1729, DOI: 10.1109/TGRS.2003.815408.

[26] Hedley, J. D.; Harborne, A. R.; Mumby, P. J. Simple and robust removal of sun glint for mapping shallow-water benthos. *International Journal of Remote Sensing* **2007,** *Volume 26*, pp. 2107 – 2112, DOI: 10.1080/01431160500034086.

[27] Lyzenga, D. Passive Remote Sensing Techniques for Mapping Water Depth and Bottom Features. *Applied Optics* **1978**, *Volume 17*, pp. 379 – 383, DOI: 10.1364/AO.17.000379.

[28] Stumpf, R.; Holderied, K. Determination of Water Depth with High-Resolution Satellite Imagery Over Variable Bottom Types. *Liminology and Oceanography* **2003**, pp. 547 – 556, DOI: 10.4319/lo.2003.48.1_part_2.0547.

[29] Maltese, A.; Pampalone, V.; Malthus, T. J.; Ciraolo, G.; Karpouzil, E.; Loggia, G. L. Processing of Field Spectroradiometric Data For Remote Sensing Mapping of Submerged Vegetation in Coastal Zones and Lagoon Environments. *EARSeL eProceedings* **2009**, *Volume* 7, pp. 105 – 119.

[30] Yang, C. The Empirical Models to Correct Water Column Effects for Optically Shallow Water. In *Empirical Modeling and Its Applications*; Habib, M., Ed.; InTech, 2016, ISBN 978-953-51-2494-8.

[31] Zaffoli, M. L.; Frouin, R.; Kampel, M. Water Column Correction for Coral Reef Studies by Remote Sensing *Sensors* **2014**, *Volume 14,* pp. 16881 – 16931, DOI: 10.3390/s140916881.

[32] Misbari, S.; Hashim, M. Change Detection of Submerged Seagrass Biomass in Shallow Coastal Water *Remote Sensing* **2016,** *Volume 8*, pp. 200, DOI: 10.3390/rs8030200.

[33] Giardino, C.; Candiani, G.; Bresiani, M.; Lee, Z.; Gagliano, S.; Pepe, M. BOMBER: A Tool for Estimating Water Quality and Bottom Properties from Remote Sensing. *Computer and Geosciences* **2012,** *Volume 45*, pp. 313-318, DOI: 10.1016/j.cageo.2011.11.022.

[34] Albert, A.; Mobley, C. D. An Analytical Model for Subsurface Irradiance and Remote Sensing Reflectance in Deep and Shallow Case-2 Waters. *Optics Express* **2003**, *Volume* 11, pp 2873 – 2890.

[35] Lee, Z.; Carder, K. L.; Mobley, C. D.; Steward, R. G.; Patch, J. S. Hyperspectral Remote Sensing for Shallow Waters: 1. A Semianalytical Model. *Applied Optics* **1998**, *Volume* 37, pp. 6329 – 6338, DOI: 10.1364/AO.37.006329

[36] Yang, C.; Yang, D.; Cao, W.; Zhao, J.; Wang, G.; Sun, Z.; Xu, Z.; Ravi Kumar, M. S. Analysis of seagrass reflectivity by using a water column correction algorithm. *International Journal of Remote Sensing* **2010**, *Volume* 31, pp. 4595 – 4608, DOI: 1080/01431161.2010.485138